

Effects of Charge Fluctuation on Two-Membrane Instability and Fusion

Yong Woon Kim* and Wokyung Sung

Department of Physics, Pohang University of Science and Technology, Pohang 790-784, South Korea
(Received 23 October 2002; published 9 September 2003)

Membrane fusion is fundamental to diverse biological processes ranging from intercellular and intracellular transport to egg fertilization. We study the effects of coupling between membrane undulation and charge fluctuation on its fusion. We find that, at concentrations of millimolar range, multivalent cations such as calcium in solution induce a strong correlated-charge fluctuation on each membrane, leading to inversion and overcondensation of surface charges. When the charge fluctuation is cooperatively coupled to undulation, two apposing membranes undergo a dynamic instability to spontaneous growth of in-phase undulation with submicron wavelengths, thereby greatly reducing fusion barrier.

DOI: 10.1103/PhysRevLett.91.118101

PACS numbers: 87.16.Dg, 61.20.Qg, 87.15.He, 87.15.Ya

Every cell and its internal compartments are enclosed by bilayer membranes. Thus, membrane fusion occurs continuously in a living cell during a wide variety of processes encompassing exocytosis, endocytosis, intracellular trafficking, and viral infection [1]. It is also a central step in biotechnology of targeted drug delivery and gene therapy. However, quantitative explanation of this fundamental phenomenon on physical grounds is yet lacking due to complexities of biomembrane architectures and diversities of fusion pathways. To elucidate and distill generic principles behind fusion, model lipid vesicles or liposomes with simple and well-defined constituents have been extensively studied [2,3]. A universal feature among important aspects hitherto accumulated is that vesicles of various types start to fuse above a threshold concentration of divalent cations in solution, usually in millimolar range [4–6]. Motivated by these observations, we investigate the effects of the multivalent cations, Ca^{2+} in particular, on the dynamics of two apposing flexible membranes.

It is known that the initial stage of membrane fusion consists of two kinetic steps; membranes first aggregate to form a stable bound state (adhesion), followed by the second process, merging of two membranes. For two identical, flat and uniformly charged membranes placed to be parallel with a distance z , intermembrane potential energy $V(z)$ is well known [7], looking like Fig. 1(a) in view of one membrane with the other located at $z = 0$. $V(z)$ has a barrier, $\Delta V = V(z = 0)$, mostly due to hydration repulsion and, typically a well, due to balance between van der Waals attraction and electrostatic repulsion. Near the potential minimum, characterized by separation d and curvature $\Omega = d^2 V/dz^2|_{z=d}$, $V(z)$ is approximated as $-V_0 + \frac{1}{2}\Omega(z-d)^2$, where Ω can also incorporate the steric repulsion at the distance d of a few nanometers. We consider that two identical membranes composed of anionic and neutral lipids with average, negative charge density $-\sigma_0$ are immersed in a salty solution including multivalent ions. Multivalent cations in the solution tend to dominantly adsorb (condense) within a

thin diffusive layer on a negatively charged surface. This cation condensation modifies surface charge density as $\sigma = -\sigma_0 + \sum_Z Z n_Z$, where n_Z is number density of adsorbed counterions with valency Z . The adsorption and subsequent desorption of the individual counterions within the layer, along with lateral diffusion of the charged lipids, allow spatial and temporal fluctuations of σ . Now suppose the two membranes are initially brought to the state of adhesion, oscillating about the separation $z = d$, and then ask what follows for the process of merging. An interesting effect of the charge fluctuation is that the charge distribution on one object is likely to rearrange itself in correlation with that on the other, leading to an unusual consequence of attraction between like-charged objects [8,9]. However, this attraction between membranes [10,11] is known to be not strong enough to overcome a huge repulsion barrier as typically high as $\Delta V \approx 24k_B T/\text{nm}^2$ [7]. As an important attribute to fusion, we explore the charge fluctuation induced by the multivalent cations, which can be stronger than commonly thought. Another substantial feature we incorporate is that the membranes are flexible and exhibit thermally induced shape fluctuation due to their fluidity. A planar membrane thermally undulates in response to variations of the charge distributions which, in turn, rely

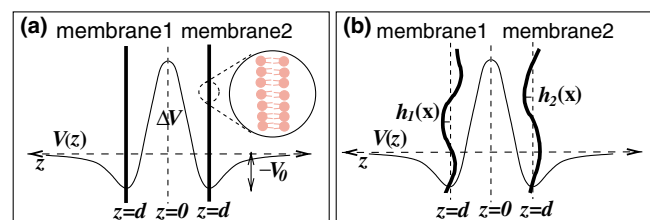


FIG. 1 (color online). Two planar membranes can form an adhesion state under intermembrane potential $V(z)$ with an average separation d . (a) Thick lines indicate the center lines of two parallel membranes composed of lipid bilayers (circle). (b) The wiggling curves represent the center lines of the membranes with thermal undulations $h_i(\mathbf{x})$ ($i = 1, 2$).

on the membrane configuration. In this Letter, we show that the membrane undulation can cooperatively couple with the correlated-charge fluctuation enhanced by the multivalent counterions to greatly reduce the fusion barrier.

Now let us formulate free energy associated with the fluctuations and their dynamics. The effective surface charge density of each membrane $i = 1, 2$ has fluctuation $\delta\sigma_i(\mathbf{x})$ around its average value $\bar{\sigma}$, $\sigma_i(\mathbf{x}) = \bar{\sigma} + \delta\sigma_i(\mathbf{x})$. On the other hand, noncondensed, free ions from the solution contribute to screening the Coulomb interactions among the surface charges. Local membrane undulations $h_i(\mathbf{x})$ are measured over the reference planes with two-dimensional coordinate $\mathbf{x} = (x, y)$ [see Fig. 1(b)] on which the projected densities $\sigma_i(\mathbf{x})$ are defined [12]. In view of the figure, each membrane within the adhesion well has the effective free energy,

$$\mathcal{F}_i = \frac{1}{2} \int d^2\mathbf{x} d^2\mathbf{x}' \sigma_i(\mathbf{x}) \sigma_i(\mathbf{x}') v(\mathbf{x} - \mathbf{x}', h_i(\mathbf{x}) - h_i(\mathbf{x}')) + \frac{1}{2} \int d^2\mathbf{x} [\chi(\delta\sigma_i(\mathbf{x}))^2 + \kappa(\nabla_{\mathbf{x}}^2 h_i(\mathbf{x}))^2 + \Omega h_i(\mathbf{x})^2]. \quad (1)$$

The first term represents the screened Coulomb interaction between effective charges on membrane i , where $v(\mathbf{x}, z) = \exp(-\kappa_D \sqrt{\mathbf{x}^2 + z^2}) / \epsilon \sqrt{\mathbf{x}^2 + z^2}$. The ionic solution has dielectric constant ϵ and inverse of Debye screening length κ_D . The second term signifies entropy loss [12,13] caused by density fluctuation of the magnitude parametrized by χ . The third term denotes the energy cost of membrane undulations with a bending rigidity κ . The last term stands for confining effects on undulations in the adhesion well [14]. Apart from an irrelevant additive constant, total free energy of two membranes is $\mathcal{F} = \mathcal{F}_1 + \mathcal{F}_2 + \mathcal{F}_{12}$, with the intermembrane electrostatic interaction \mathcal{F}_{12} given by [15]

$$\mathcal{F}_{12} = \int d^2\mathbf{x} d^2\mathbf{x}' \sigma_1(\mathbf{x}) \sigma_2(\mathbf{x}') \times v(\mathbf{x} - \mathbf{x}', d + h_1(\mathbf{x}) - h_2(\mathbf{x}')). \quad (2)$$

The dynamics of $\delta\sigma_i$ can be obtained by the fluctuating diffusion equation (Cahn-Hilliard model) [16] in the Fourier space,

$$\frac{\partial}{\partial t} \delta\sigma_{i\mathbf{q}} = -Dq^2 \left(\frac{\partial \mathcal{F}}{\partial \delta\sigma_{i\mathbf{q}}} \right) + \zeta_{i\mathbf{q}}(t), \quad (3)$$

where $\delta\sigma_{i\mathbf{q}} = \int d\mathbf{x} e^{-i\mathbf{q}\cdot\mathbf{x}} \delta\sigma_i(\mathbf{x})$ is the Fourier transform of $\delta\sigma_i(\mathbf{x})$, D is an Onsager coefficient, $q = |\mathbf{q}|$, and $\zeta_{i\mathbf{q}}(t)$ is a random thermal noise. The undulations disturb the ambient viscous fluid, and vice versa, which we describe hydrodynamically. The fluid flow, regarded as incompressible, causes intramembrane and intermembrane hydrodynamic interactions [14]. Change of h_i in time,

assumed to be identical to the fluid velocity normal to the surface, is governed by

$$\frac{\partial}{\partial t} \begin{pmatrix} h_{1\mathbf{q}} \\ h_{2\mathbf{q}} \end{pmatrix} = -\frac{1}{4\eta q} \begin{pmatrix} A_1 & A_2 \\ A_2 & A_1 \end{pmatrix} \begin{pmatrix} \partial \mathcal{F} / \partial h_{1\mathbf{q}}^* \\ \partial \mathcal{F} / \partial h_{2\mathbf{q}}^* \end{pmatrix} + \begin{pmatrix} \xi_{1\mathbf{q}}(t) \\ \xi_{2\mathbf{q}}(t) \end{pmatrix}, \quad (4)$$

where η is fluid shear viscosity, A_i are coefficients given as functions of qd [17], and $\xi_{i\mathbf{q}}$ is a random thermal noise. Through thermal noises, ξ and ζ , the initially nonequilibrium system reaches the equilibrium state of minimum free energy after a long time.

Expanding \mathcal{F} up to bilinear order (Gaussian level) of $\delta\sigma_{i\mathbf{q}}$ and $h_{i\mathbf{q}}$, their dynamic equations, Eqs. (3) and (4), become linear:

$$\frac{\partial}{\partial t} \mathbf{X} = -\Gamma \cdot \mathbf{X} + \mathbf{Y}, \quad (5)$$

where $\mathbf{X} = (h_{1\mathbf{q}}, h_{2\mathbf{q}}, \delta\sigma_{1\mathbf{q}}, \delta\sigma_{2\mathbf{q}})^\dagger$ and $\mathbf{Y} = (\xi_{1\mathbf{q}}, \xi_{2\mathbf{q}}, \zeta_{1\mathbf{q}}, \zeta_{2\mathbf{q}})^\dagger$. Dynamic coupling between the four relevant variables is described by 4×4 matrix Γ that depends upon the parameters of systems as well as q [17]. The collective dynamical modes arising from the coupling are determined by four eigenvectors and eigenvalues of Γ . As shown in Fig. 2, we find that, using representative parameters, one of the four eigenvalues, denoted by γ , is negative in a narrow range around the minimum point, $q_m \approx 0.07 \text{ nm}^{-1}$. It occurs provided the membranes are overcharged so that the absolute value of $\bar{\sigma}$ is larger than a critical value σ^* , the details of which

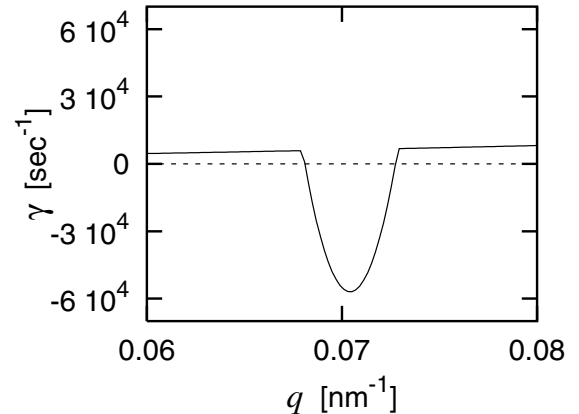


FIG. 2. An eigenvalue γ of Γ can be negative within a small range around $q_m \approx 0.07 \text{ nm}^{-1}$. The parameters we used are $\kappa = 10k_B T$, $\eta = 10^{-2} \text{ ergs/cm}^3$, and $D = 10^5 e^2 / k_B T \text{ s}$. For membranes with $-\sigma_0 = -0.3e/\text{nm}^2$ in a solution of 0.1 M NaCl added with 4 mM Ca^{2+} , $\bar{\sigma} = 0.22e/\text{nm}^2$, above σ^* (self-consistent determination of $\bar{\sigma}$ and role of Ca^{2+} will be discussed next; see also Fig. 4). To determine Ω and d , we, along with the screened Coulomb interaction with surface charge density $\bar{\sigma}$, incorporate hydration and van der Waals interaction; $V_{\text{hyd}} = V_h e^{-z/a}$ and $V_{\text{vdw}} = -H/12\pi z^2$, where $V_h = 0.1 \text{ J/m}^2$, $a = 2 \text{ \AA}$, and Hamaker constant $H = 10^{-20} \text{ J}$ (adopted from Ref. [7]).

will be discussed shortly. Existence of a negative eigenvalue signals the onset of a dynamic instability where the corresponding eigenmode with q in the particular range grow exponentially ($\sim e^{|\gamma|t}$) in time. This eigenmode takes the form of $(u, u, w, -w)^\dagger$, indicating in-phase intermembrane coherence in height undulation (u, u) along with out-of-phase coherence in charge modulations $(w, -w)$, with common wavelengths around $\lambda = 2\pi/q_m \approx 90$ nm. Here u and w are functions of q as well as the parameters presented in Fig. 2 [17]. It is noted that the induced wavelength here is quite large compared to the membrane separation d , $q_m d < 1$.

An argument below illustrates the physical mechanism underlying the process of dynamic instability (Fig. 3). Initially two identical, overcharged membranes approach and form an adhesion state with an average distance d [Fig. 3(a)]. In the course of time, the surface charges in a membrane, subject to net-charge conservation, redistribute in correlation with those in the other to induce the electrostatic attraction as shown in Fig. 3(b), if the membrane were to remain planar. Because of the bending flexibility, however, this out-of-phase charge (intermembrane) correlation can be accompanied by the in-phase undulation coherence as shown in Fig. 3(c). This leads to further reduction of the electrostatic interaction energy on curved surfaces not only by bringing unlike charges across membranes closer, but also by leaving majorities of like charges more separated than on flat surfaces. For unstable undulation wavelengths λ of the range indicated in Fig. 2, these correlated undulation and charge distribution will gradually grow [Fig. 3(d)] within validity of our linear dynamics model. For undulation with the other values of wavelength, such a cooperative coupling would not occur, but the membranes will relax fast to stable planar configurations. The free energy reduction $\Delta\mathcal{F}$ due to the unstable mode can be very large so as to offset the energy barrier ΔV . From $\Delta\mathcal{F} = \Delta\mathcal{F}_0 e^{2|\gamma|t}$ as a result of Gaussian fluctuations, we can estimate the time for the

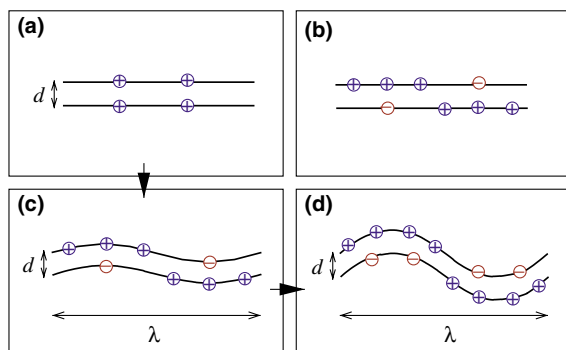


FIG. 3 (color online). Schematic pictures explaining the mechanism of dynamical instability, (a) \rightarrow (c) \rightarrow (d). Thick parallel lines are average center lines of two membranes at adhesion, and circled signs represent effective surface charges of membranes.

two membranes to cross the barrier, i.e., merge, as $\tau = \ln(|\Delta V/\Delta\mathcal{F}_0|)/(2|\gamma|)$, which is of the order of $|\gamma|^{-1} \sim 1$ msec, largely independent of the energy barrier. Remarkably, this estimate agrees with the experimental values of fusion time.

Recently, dynamical instability of a single membrane was reported to occur due to charge accumulation on crests of bilayer, irrespective of q for tension-free membrane [18]. On the other hand, two-membrane instability predicted here takes place only in a narrow range of q . This is a consequence of the cooperative coupling of hydrodynamic and electrostatic interactions in the intervening watery medium. We note that strong overcharging to yield large $\bar{\sigma}$ is required for the instability, because it is driven not only by the attraction between unlike charges on adjacent membranes but also by the repulsion between like charges on each membrane [12].

We now discuss the mechanism that underlies the overcharging and the role played by the multivalent cations such as Ca^{2+} . When the membranes are in a solution of only monovalent ions such as NaCl, $\bar{\sigma}$ becomes $-\sigma_0 + e\bar{n}_1$, which is assumed to be below σ^* for the membranes to be stable. It is further changed into $\bar{\sigma} = -\sigma_0 + e\bar{n}_1 + 2e\bar{n}_2$ after addition of divalent counterions such as Ca^{2+} . Given $-\sigma_0$ and the bulk ionic concentrations, $\bar{\sigma}$ should be determined self-consistently by considering the phase equilibria between counterions on the surface and in the bulk. To evaluate the equilibrium values of \bar{n}_Z ($Z = 1, 2$), and thus $\bar{\sigma}$, we consider two uniformly charged parallel

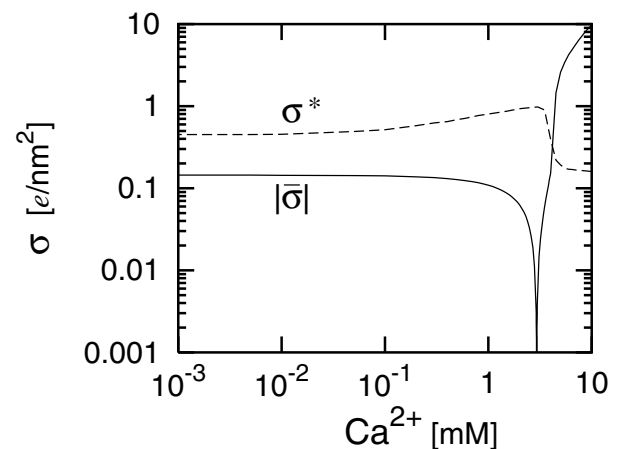


FIG. 4. Absolute value of the average effective surface charge density $\bar{\sigma}$ (solid line) and the critical density σ^* (dashed line) as a function of calcium concentration in mM. We consider two apposed membranes with $-\sigma_0 = -0.30e/\text{nm}^2$ embedded in a solution of 0.1 M NaCl, resulting in $\bar{\sigma} = -0.14e/\text{nm}^2$ in the absence of Ca^{2+} , whose magnitude is below σ^* . With the addition of cations to $[\text{Ca}^{2+}] = 3$ mM, the condensed counterions neutralize the negative bare charges completely (downward cusp in the figure), leading to the charge inversion and, upon addition of 4 mM Ca^{2+} , $\bar{\sigma}$ increases to $+0.22e/\text{nm}^2$ just above σ^* .

surfaces with adsorbing counterions, and in-plane charge fluctuations up to bilinear order in the free energy. The chemical potential of condensed counterions μ_Z^{cond} comes from derivatives of the free energy with respect to \bar{n}_Z , and that of free counterions μ_Z^{free} is for simplicity assumed to be the ideal gas entropy by neglecting the Coulomb energy due to their low densities. Using the phase equilibria conditions, $\mu_Z^{\text{cond}} = \mu_Z^{\text{free}}$ ($Z = 1, 2$), we obtain Fig. 4, which shows the changes of absolute value of $\bar{\sigma}$ and threshold value σ^* as a function of bulk calcium concentration for the membranes of $-\sigma_0 = -0.3e/\text{nm}^2$ in 0.1 M NaCl solution. We find $\bar{\sigma} = -0.14e/\text{nm}^2$ for the membrane in the solution with NaCl only, but upon 4 mM calcium entry, $\bar{\sigma}$ is changed into $+0.22e/\text{nm}^2$ above $\sigma^* = 0.21e/\text{nm}^2$. One notable feature, observed typically over a range of σ_0 , is that Ca^{2+} in the millimolar range gives rise to surface charge overcondensation preceded by charge inversion to positivity (Fig. 4). The underlying physics can be explained as follows. As the bulk concentration of divalent cations increases, they undergo enhanced counterion condensation and charge fluctuation, suffering from a pronounced correlation-induced attraction to the membranes. This attraction in turn reinforces the additional counterion condensation even after net-charge neutralization and thus bring about overcondensation with large $\bar{\sigma}$. Since the charge-correlation contribution to μ_Z^{cond} is found to be prominently proportional to $-Z^2/\chi$, the presence of multivalent counterions is essential for the overcharging. Despite their relatively high concentrations, the monovalent salts cannot therefore inverse but screen the surface charges. We note this case presents a novel example of giant charge inversion [19] induced by thermal fluctuation. In short, the $|\bar{\sigma}|$ can exceed σ^* upon Ca^{2+} influx of millimolar range, and then the initially stable membranes in the presence of only the monovalent counterions become unstable. Our results are consistent with the experimental observations [4–6] and unambiguously explain the role of multivalent cations like Ca^{2+} in fusion. As additional evidence of the strong multivalency effect, we also find discontinuous charge inversion upon the addition of trivalent ions of μM range, which seems to be in accord with a recent theoretical result [20] and with fusion experiments using La^{3+} and Tb^{3+} [4]. Although our analysis is based on the Gaussian approximation, the physical picture drawn above can be a quintessence for future studies.

In summary, we have investigated a dynamical instability of two membranes where charge fluctuation and membrane undulation cooperatively play a key role. For calcium concentration above a threshold, two approaching negatively charged vesicles can spontaneously form discernible ripples that grow within apposed regions to overcome the fusion barrier otherwise too high to surmount. The present work gives an appealing physical insight into the nonspecific action of calcium, consistent

with some experimental observations, and suggests new experiments for future studies, e.g., giant charge inversion and ripple formation at the onset of fusion.

The authors thank D.S. Koh for helpful discussions. This work was supported by KRF (DS0008), National RND program by MOST (M10214000230), and by POSTECH BSRI (IRB021081).

*Present address: Sektion Physik, LMU München, Theresienstrasse 37, 80333 München, Germany.

- [1] B. Albert *et al.*, *Molecular Biology of the Cell* (Garland, New York, 1994).
- [2] J. Wilschut, in *Membrane Fusion*, edited by J. Wilschut and D. Hoekstra (Marcel Dekker, New York, 1991).
- [3] F. Szokz, in *Cell Fusion*, edited by A. E. Sowers (Plenum, New York, 1987).
- [4] K. Arnold, in *Structure and Dynamics of Membranes*, edited by R. Lipowsky and E. Sackmann (Elsevier, Amsterdam, 1995), Vol. 2.
- [5] D. Papahadjopoulos *et al.*, in *Molecular Mechanisms of Membrane Fusion*, edited by S. Ohki *et al.* (Plenum, New York, 1988).
- [6] S. Ohki, in *Cell and Model Membrane Interactions*, edited by S. Ohki (Plenum, New York, 1991).
- [7] J. N. Israelachvili, *Intermolecular and Surface Forces* (Academic, San Diego, 1992).
- [8] N. Grønbech-Jensen, R. J. Mashl, R. F. Bruinsma, and W. M. Gelbart, *Phys. Rev. Lett.* **78**, 2477 (1997); S. Marcelja, *Biophys. J.* **61**, 1117 (1992); V. A. Bloomfield, *Biopolymers* **31**, 1471 (1991).
- [9] B.-Y. Ha and A. J. Liu, *Phys. Rev. Lett.* **79**, 1289 (1997); **81**, 1011 (1998); R. Podgornik and V. A. Parsegian, *Phys. Rev. Lett.* **80**, 1560 (1998); B. I. Shklovskii, *Phys. Rev. Lett.* **82**, 3268 (1999).
- [10] P. A. Pincus and S. A. Safran, *Europhys. Lett.* **42**, 103 (1998).
- [11] A. G. Moreira and R. R. Netz, *Phys. Rev. Lett.* **87**, 078301 (2001).
- [12] Y. W. Kim and W. Sung, *Europhys. Lett.* **58**, 147 (2002).
- [13] A. W. C. Lau and P. Pincus, *Phys. Rev. Lett.* **81**, 1338 (1998).
- [14] M. Kraus and U. Seifert, *J. Phys. II (France)* **4**, 1117 (1994); F. Brochard and J. F. Lennon, *J. Phys. (France)* **36**, 1035 (1975).
- [15] Here we assume that both the van der Waals attraction and hydration repulsion are independent of the fluctuating fields, charge fluctuations, and undulations.
- [16] P. M. Chaikin and T. C. Lubensky, *Principles of Condensed Matter Physics* (Cambridge University Press, Cambridge, England, 1995).
- [17] Y. W. Kim, Ph.D. thesis, Pohang University of Science and Technology, 2002.
- [18] V. Kumaran, *Phys. Rev. Lett.* **85**, 4996 (2000).
- [19] T. T. Nguyen, A. Y. Grosberg, and B. I. Shklovskii, *Phys. Rev. Lett.* **85**, 1568 (2000);
- [20] A. W. C. Lau, D. B. Lukatsky, P. Pincus, and S. A. Safran, *Phys. Rev. E* **65**, 051502 (2002).